Available online at www.sciencedirect.com
SCIENCE DIRECT
Journal of Solid State Chemistry 179 (2006) 2079–2085
JOURNAL OF SOLID STATE CHEMISTRY
www.elsevier.com/locate/jssc

Magnetic susceptibility and specific heat of uranium double perovskite oxides Ba_2MUO_6 (M = Co, Ni)

Yukio Hinatsu*, Yoshihiro Doi

Division of Chemistry, Graduate School of Science, Hokkaido University, Sapporo 060-0810, Japan

Received 2 December 2005; received in revised form 22 March 2006; accepted 26 March 2006
Available online 4 April 2006

Abstract

Double perovskites Ba_2MUO_6 (M = Co, Ni) were prepared by the solid-state reaction. X-ray diffraction measurements show that both cobalt (nickel) and uranium ions are ordered in the NaCl type over the six-coordinate B sites of the perovskite ABO_3. Detailed magnetic susceptibility and specific heat measurements show that Ba_2CoUO_6 and Ba_2NiUO_6 order ferromagnetically at 9.1 and 25 K, respectively. From the analysis of the magnetic specific heat, the ground states of the Co^{2+} and Ni^{2+} ions were determined.

Keywords: Magnetic properties; Uranium; Oxide; Cobalt; Nickel; Perovskite; Magnetic susceptibility; Specific heat

1. Introduction

The perovskite-type oxides have the general formula ABO_3, in which A represents a large electropositive cation, and B represents a small electropositive cation. The perovskite structure can be described as a framework of corner-sharing BO_6 octahedra which contains A cations at 12-coordinate sites. This perovskite-type oxides ABO_3 incorporate various kinds of tetravalent ions at the B site of the crystal when A is Ba or Sr. In ABO_3 perovskites, the octahedrally coordinated B cation can be substituted partially by other suitable ions. One interesting feature is that "double" perovskites $A_2M^{3+}M^{5+}O_6$ (or $A_2M^{2+}M^{6+}O_6$) are formed by replacing the +4 cations in the $A^{2+}M^{4+}O_3$ perovskite compounds with +3 and +5 cations (or +2 and +6 cations). Since the B cations generally determine the physical properties of the perovskite ABO_3 [1], the elucidation of the arrangement and position of the B cations in the double perovskite are essential to know its properties. There are three B-cation sublattice types: random, rock salt, and layered [2]. The B cations in different oxidation states often regularly order, i.e., 1:1 arrangement of M^{3+} and M^{5+} (or M^{2+} and M^{6+}) ions has been observed over the six-coordinate B sites [2–17].

Some members of the double perovskites family have been proposed as half-metallic ferromagnets, with potential applications in the emerging field of spintronics [18,19]. The prototypical example is Sr_2FeMoO_6, which was shown to exhibit intrinsic tunneling-type magneto-resistance (TMR) at room temperature [18]. Further studies on the Ca, Ba analogs of the Sr_2FeMoO_6 showed that both the Ca_2FeMoO_6 and Ba_2FeMoO_6 also exhibited semi-metallic and ferromagnetic properties [19,20]. The Co analogs of Sr_2FeMO_6 (M = Mo, W) also indicate the occurrence of the magneto-resistance [21].

Pinacca et al. [22] reported the magnetic properties for the uranium analog of the double perovskite Sr_2CoMO_6, i.e., Sr_2CoUO_6. A canted antiferromagnetic structure was observed below $T_N = 10$ K, with an ordered magnetic moment of 2.44(7) μ_B for Co^{2+} ions. The effective magnetic moment calculated from the Curie–Weiss law at high temperatures indicates that the orbital contribution to the magnetic moment was unquenched at high temperatures. Magnetic and structural features were consistent with an electronic configuration Co^{2+} [$3d^7$]–U^{6+} [Rn] ([Rn]: radon electronic core).

Previously, we prepared Ba_2MUO_6 with M = Co and Ni, and reported their magnetic properties through magnetic

*Corresponding author. Fax: +81 11 706 2702.
E-mail address: hinatsu@sci.hokudai.ac.jp (Y. Hinatsu).

0022-4596/$ - see front matter © 2006 Elsevier Inc. All rights reserved.
doi:10.1016/j.jssc.2006.03.037

susceptibility measurements. Ba_2CoUO_6 and Ba_2NiUO_6 show a ferromagnetic behavior below 9 and 25 K, respectively [23]. This result is contrastive with the result for Ba_2CoWO_6 and Ba_2NiWO_6, i.e., these are antiferromagnetic with $T_N = 17$ and 55 K, respectively [24].

In order to obtain further information about the crystal structure and magnetic properties for these Ba_2CoUO_6 and Ba_2NiUO_6, we have performed X-ray diffraction, magnetic susceptibility, and specific heat measurements. Their results will be discussed here.

2. Experimental

Samples were prepared by solid-state reactions. As starting materials, $BaCO_3$, CoO (or NiO), and U_3O_8 were used. Before use, $BaCO_3$ was heated in atmosphere at 800 °C to remove any moisture and U_3O_8 was oxidized in air at 850 °C to form the stoichiometric compound. $BaCO_3$, CoO (or NiO) and U_3O_8 were weighed in the intended stoichiometric metal ratio Ba:Co(Ni):U = 2:1:1. After being finely ground in an agate mortar, the mixtures were pressed into pellets and then heated in air at 1000 °C for 120 h with several intermediate re-grindings.

Powder X-ray diffraction profiles were measured using a Rigaku Multi-Flex diffractometer with Cu$K\alpha$ radiation equipped with a curved graphite monochromator. The data were collected by step scanning in the angle range of $10° \leqslant 2\theta \leqslant 120°$ at a 2θ step size of 0.02°. The X-ray diffraction data were analyzed by the Rietveld technique, using the programs RIETAN2000 [25].

The temperature dependence of the magnetic susceptibility was measured with a SQUID magnetometer (Quantum Design, MPMS) under both zero-field-cooled (ZFC) conditions and field-cooled (FC) conditions. The former was measured on heating the sample up to 400 K under the applied magnetic field of 0.1 T after zero-field cooling to 1.8 K. The latter was measured upon cooling the sample from 400 to 1.8 K under 0.1 T. The field dependence of magnetization was measured at 5 K over the applied magnetic field range of $-5\,T \leqslant H \leqslant 5\,T$.

The specific heats were measured using a relaxation technique applied by a specific heat measuring system (Quantum Design, PPMS) in the temperature range of $1.8 \leqslant T \leqslant 300$ K. The sample in the form of a thin plate was mounted on a sample holder (thin alumina plate) with Apiezon for better thermal contact.

3. Results and discussion

3.1. Preparation and crystal structure

Figs. 1(a) and (b) show the X-ray diffraction profiles for Ba_2CoUO_6 and Ba_2NiUO_6, respectively. The X-ray

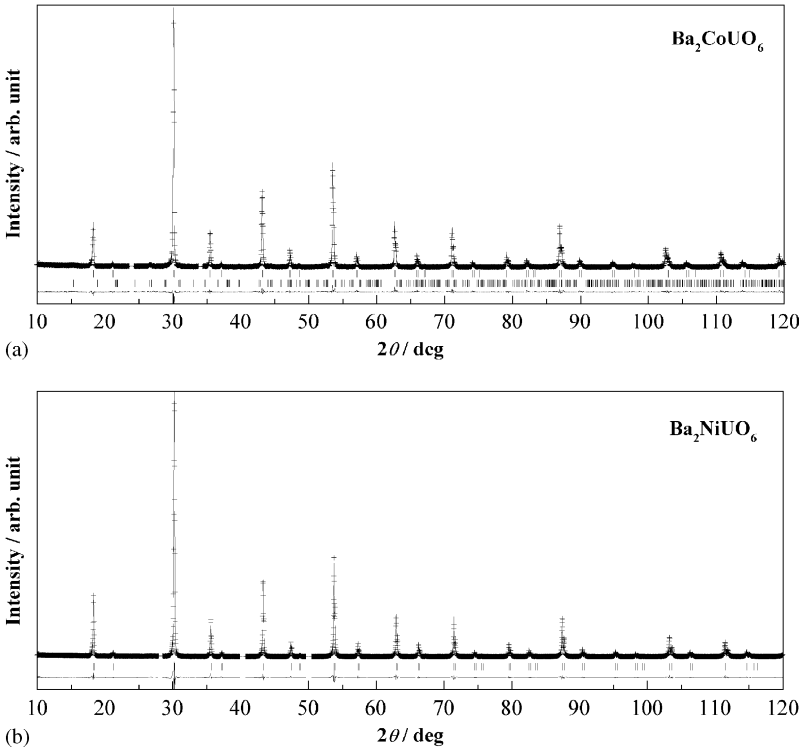

Fig. 1. Powder X-ray diffraction profiles for (a) Ba_2CoUO_6 and (b) Ba_2NiUO_6. The calculated and observed profiles are shown on the top solid line and cross markers, respectively. The vertical marks in the middle show positions calculated for Bragg reflections. The lower trace is a plot of the difference between calculated and observed intensities. For (a) Ba_2CoUO_6, the second vertical marks in the middle show positions calculated for Bragg reflections of the impurity $BaUO_4$ (see text).

diffraction measurements showed that both compounds were crystallized in a cubic phase. We have performed the Rietveld analysis for the X-ray diffraction profiles. As another compound $BaUO_4$ was detected as a minor impurity in the diffraction profile for Ba_2CoUO_6, it was included as a second phase in the refinement. From the scale factors, the amount of $BaUO_4$ in the sample was 1.6%. In the diffraction profile for Ba_2NiUO_6, some very weak unidentified diffraction lines were detected. They were excluded from the Rietveld analysis. The structure was refined by applying the space group $Fm\bar{3}m$. This space group allows two crystallographically distinct octahedral sites in the perovskite structure, thus permitting 1:1 positional ordering between the *B*-site ions, U^{6+} and Co^{2+} (or Ni^{2+}) ions. Therefore, the deviation from the cubic symmetry of the BO_6 octahedral coordination is not observed. The refined structural parameters for Ba_2CoUO_6 and Ba_2NiUO_6 are listed in Table 1. Fig. 2 shows the crystal structure of Ba_2MUO_6 (M = Co, Ni). Table 2 lists some important bond lengths. The U^{6+}–O^{2-} bond lengths (2.121(7) Å for Ba_2CoUO_6, 2.089(5) Å for Ba_2NiUO_6) are almost equal to the value estimated from the Shannon's values (2.08 Å) [26]. Bond lengths for Co^{2+}–O^{2-} (2.066(7) Å) and Ni^{2+}–O^{2-} (2.076(5) Å) also support the cobalt (nickel) ions being in the +2 state. To obtain some insight into the oxidation states distributions, we have performed bond–valence analysis according to the Brown model [27], and the results are also listed in Table 2. The values of bond–valence sums show that the ionic species in these compounds should be $Ba_2^{2+}Co^{2+}U^{6+}O_6^{2-}$ and $Ba_2^{2+}Ni^{2+}U^{6+}O_6^{2-}$. As will be described later, the results of the magnetic susceptibility measurements also show the validity for the oxidation states of Co (Ni) and U.

3.2. Magnetic properties

3.2.1. Ba_2CoUO_6

Fig. 3 shows the temperature dependence of the magnetic susceptibilities for Ba_2CoUO_6. A ferromagnetic transition is observed at 9.0 K, which corresponds to our previous results [23]. The present detailed measurements reveal the divergence between the ZFC and FC susceptibilities below this transition temperature. The solid line in the inset of Fig. 3 shows the Curie–Weiss fitting for the magnetic susceptibilities. The effective magnetic moment (μ_{eff}) and Weiss constant (θ) are calculated to be 4.98(2) μ_B and 14.7(6) K, respectively. Since the U^{6+} ion is diamagnetic, the magnetic properties of this compound

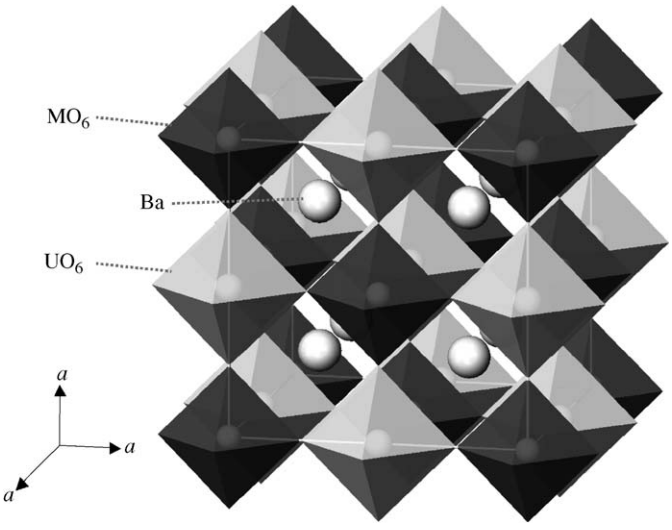

Fig. 2. The crystal structure of Ba_2MUO_6 (M = Co, Ni).

Table 1
Structural parameters for Ba_2MUO_6 (M = Co, Ni)

Atom	Site	x	y	Z	B (Å^2)
Ba_2CoUO_6					
Space group $Fm\bar{3}m$					
Ba	8*c*	1/4	1/4	1/4	0.1(1)
Co	4*b*	1/2	1/2	1/2	0.2
U	4*a*	0	0	0	0.2
O	24*e*	0.2467(8)	0	0	1.1(1)
$a = 8.3738(2)$ Å, $V = 587.18(2)$ Å^3					
$wR_p = 12.16\%$, $R_I = 4.49\%$, $R_e = 9.49\%$					
Ba_2NiUO_6					
Space group $Fm\bar{3}m$					
Ba	8*c*	1/4	1/4	1/4	0.43(6)
Ni	4*b*	1/2	1/2	1/2	0.50(7)
U	4*a*	0	0	0	0.36(5)
O	24*e*	0.2492(6)	0	0	0.73(5)
$a = 8.3311(1)$ Å, $V = 578.24(1)$ Å^3					
$wR_p = 11.20\%$, $R_I = 1.91\%$, $R_e = 6.34\%$					

Note: Definition of reliability factors wR_p, R_I and R_e are given as follows: $wR_p = \left[\sum w(|F_{(o)}| - |F_{(c)}|)^2 / \sum w|F_{(o)}|^2\right]^{1/2}$, $R_I = \sum |I_{k(o)} - I_{k(c)}| / \sum I_{k(o)}$, and $R_e = [(N-p)/\sum_i w_i y_i^2]^{1/2}$.

Table 2
Bond lengths and bond–valence sums for Ba_2CoUO_6 and Ba_2NiUO_6

	Bond lengths	Atoms	Bond–valence sums
Ba_2CoUO_6			
Ba–O	2.961(1)	Ba	1.96
Co–O	2.066(7)	Co	2.19
U–O	2.121(7)	U	5.30
Ba_2NiUO_6			
Ba–O	2.946(1)	Ba	2.04
Ni–O	2.076(5)	Ni	1.92
U–O	2.089(5)	U	5.78

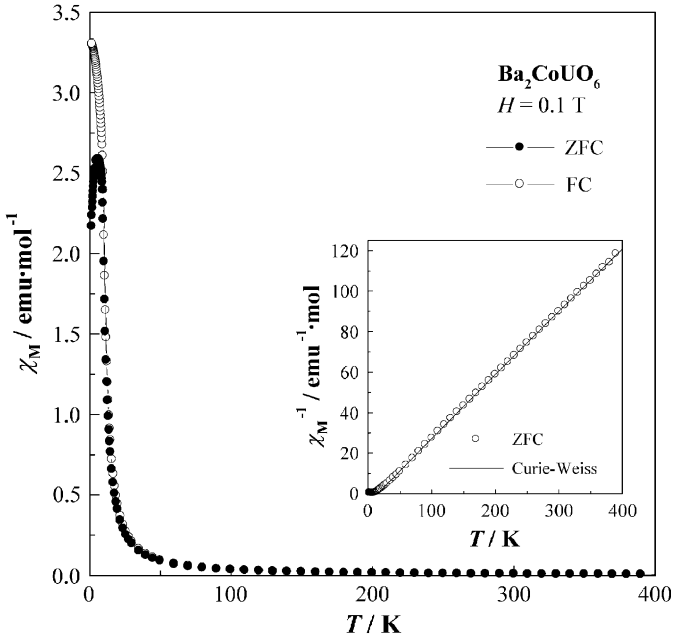

Fig. 3. Temperature dependence of the magnetic susceptibility for Ba_2CoUO_6. The inset shows the reciprocal susceptibility vs. temperature curve. The solid line is the Curie–Weiss fitting.

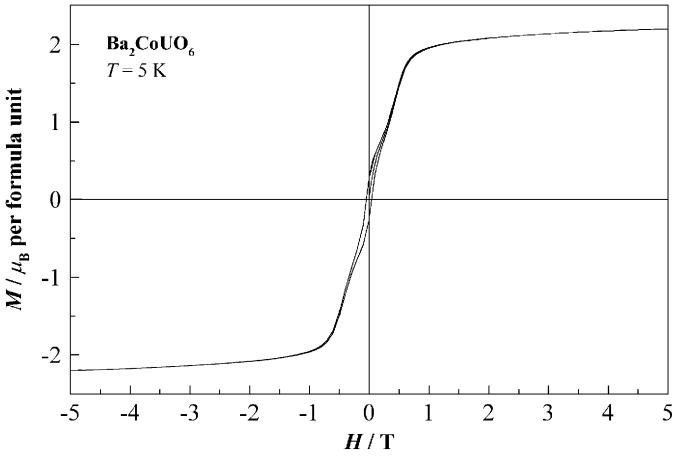

Fig. 4. Magnetic hysteresis curve for Ba_2CoUO_6 measured at 5 K.

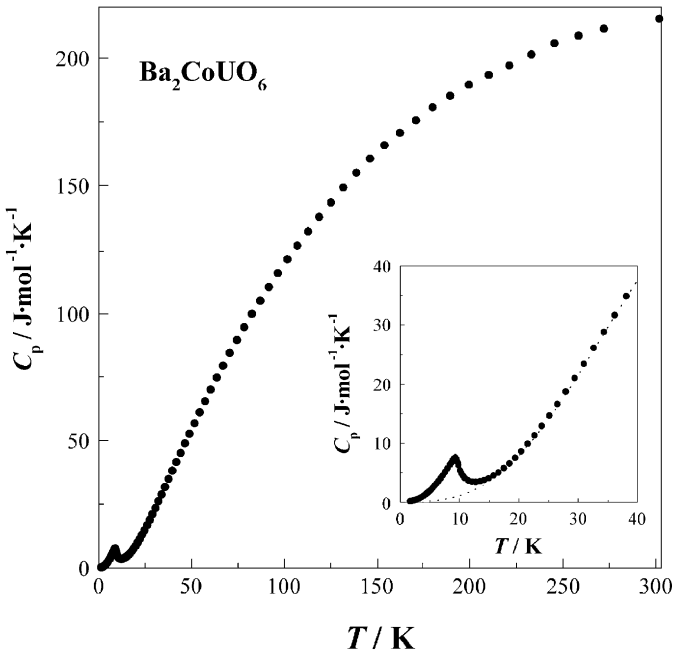

Fig. 5. Temperature dependence of the specific heat C_p for Ba_2CoUO_6. The inset shows the detailed temperature dependence below 40 K. The dotted line is the calculation results for the lattice specific heat (see text).

are due to the Co^{2+} ions. This effective magnetic moment is hardly compatible with the electronic configuration of Co^{2+} ion ([Ar]$3d^7$) and a spin-only contribution. Considering high-spin (H.S.) Co^{2+}, the total paramagnetic moment would be as low as 3.87 μ_B. High-spin octahedral Co^{2+} ion has a $^4T_{1g}$ ground state and consequently exhibits unquenched spin–orbit coupling with an expected magnetic moment of 5.20 μ_B. Usually, the octahedral Co^{2+} compounds have a moment of 4.7–5.2 μ_B [28]. That is, the experimental magnetic moment indicates that the orbital contribution to the effective magnetic moment is unquenched. And this value is quite close to the moment for $Co^{2+}U^{6+}O_4$ (4.99 μ_B) [29], and comparable moments have been reported for other double perovskites containing Co^{2+} ions [21,22,30]. The positive Weiss constant indicates the ferromagnetic interactions between Co^{2+} ions.

Fig. 4 shows the magnetization curve for Ba_2CoUO_6 at 5 K, clearly indicating a large field dependence of the magnetization and the existence of the magnetic hysteresis loop. A complete saturation of the magnetization is found and its saturation moment is 2.3 μ_B. This value is a little smaller than the moment calculated from the number of unpaired electrons, 3 μ_B. Magnetic cooperative phenomena have been reported for the similar double perovskites Ba_2CoWO_6, Ba_2NiWO_6, and Sr_2CoUO_6. Cox et al. [24] said that Ba_2CoWO_6 and Ba_2NiWO_6 showed antiferromagnetic transitions at 17 and 20 K, respectively. Pinacca et al. [22] reported Sr_2CoUO_6 to be antiferromagnetic with $T_N = 10$ K.

Fig. 5 shows the variation of the specific heat for Ba_2CoUO_6 as a function of temperature. The results of the

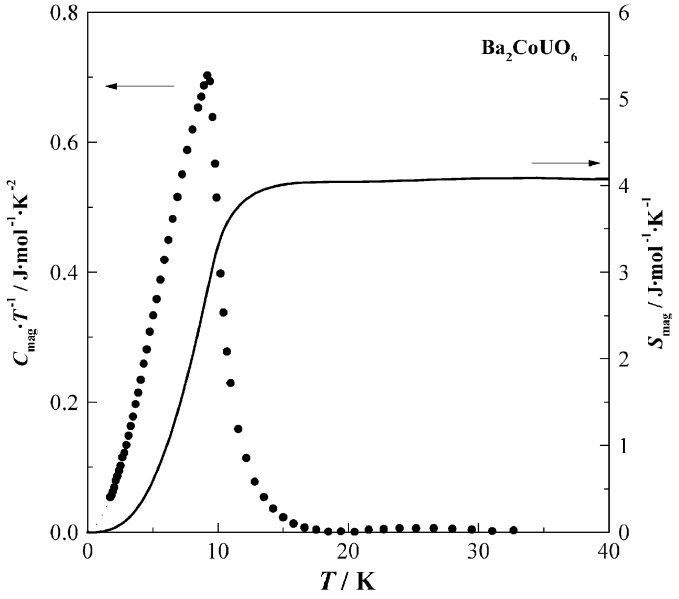

Fig. 6. Temperature dependences of the magnetic specific heat divided by temperature C_{mag}/T (left ordinate) and the magnetic entropy change S_{mag} (right ordinate) for Ba_2CoUO_6 below 40 K. The dotted line is the calculated specific heat below 1.8 K (see text).

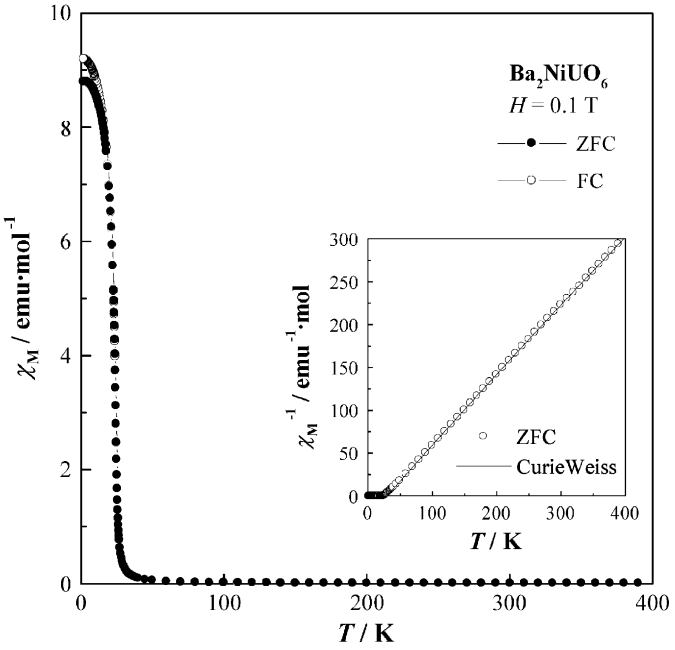

Fig. 7. Temperature dependence of the magnetic susceptibility for Ba_2NiUO_6. The inset shows the reciprocal susceptibility vs. temperature curve. The solid line is the Curie–Weiss fitting.

specific heat measurements are consistent with those of the magnetic susceptibility measurements (Fig. 3), i.e., a clear λ-type specific heat anomaly was observed at the ferromagnetic transition temperature, 9.0 K.

To calculate the magnetic contribution to the specific heat, we subtracted the lattice specific heat from the total specific heat. They were estimated by using a polynomial function of the temperature $f(T) = aT^3 + bT^5 + cT^7$ [31], in which the constants were determined by fitting this function to the observed specific heat data between 15 and 40 K. The calculated lattice specific heat is shown as a dotted curve in the inset of Fig. 5. The specific heat data below 1.8 K were extrapolated by $C_p \propto T^3$ curve [32]. The magnetic specific heat (C_{mag}) for Ba_2CoUO_6 is obtained by $C_{mag}(T) = C_p(T) - f(T)$ and its temperature dependence is shown in Fig. 6. The temperature dependence of the magnetic entropy calculated by $S_{mag}(T) = \int (C_{mag}/T)dT$ is also shown in the same figure. The magnetic entropy change due to the ferromagnetic ordering of Co^{2+} ions in the Ba_2CoUO_6 is obtained to be about 4.1 J/mol K. In general, the magnetic entropy change is expressed by the $S_{mag} = R \ln W$ (R is the molar gas constant and W the number of states for the Ln ion). The experimental value corresponds to the case for $W = 2$. The result of the magnetic entropy change indicates that the degeneracy of the ground state for the Co^{2+} ion in Ba_2CoUO_6 should be twofold.

3.2.2. Ba_2NiUO_6

Fig. 7 shows the temperature dependence of the magnetic susceptibilities for Ba_2NiUO_6. This compound also shows a ferromagnetic behavior at low temperatures and the transition temperature is about 25 K. The small divergence between the ZFC and FC susceptibilities is found below this transition temperature. The solid line in the inset of Fig. 7 shows the Curie–Weiss fitting for the magnetic susceptibility vs. temperature curve. The effective magnetic moment (μ_{eff}) and Weiss constant (θ) are calculated to be 3.07(1) μ_B and 29.7(3) K, respectively. The large positive Weiss constant shows the strong ferromagnetic interactions between Ni^{2+} ions. The magnetic properties of this compound are ascribed to the Ni^{2+} ions because the U^{6+} ion is diamagnetic. It is known that for the Ni^{2+} ion in an octahedral crystal field, the crystal field is operative and the effective magnetic moment is larger than the spin-only value calculated from the equation $\mu_{eff} = 2[S(S+1)]^{1/2}$ and is usually in the range from 2.9 to 3.5 μ_B [33,34]. The value observed experimentally (3.07(1) μ_B) is in this range, which means that the crystal field effect is operative to some extent.

A complete saturation of the magnetization for Ba_2NiUO_6 is easily observed. Fig. 8 shows the magnetization curve as a function of applied magnetic field. The saturation moment for Ba_2NiUO_6 is 2.1 μ_B. This value is reasonable, because the moment calculated from the number of unpaired electrons is 2 μ_B.

Fig. 9 shows the variation of the specific heat for Ba_2NiUO_6 as a function of temperature. A clear λ-type specific heat anomaly was observed at the ferromagnetic transition temperature, 25 K.

The magnetic specific heat (C_{mag}) for Ba_2NiUO_6 is obtained in the same way as the case for Ba_2CoUO_6, i.e., by subtracting the calculated lattice specific heat from the

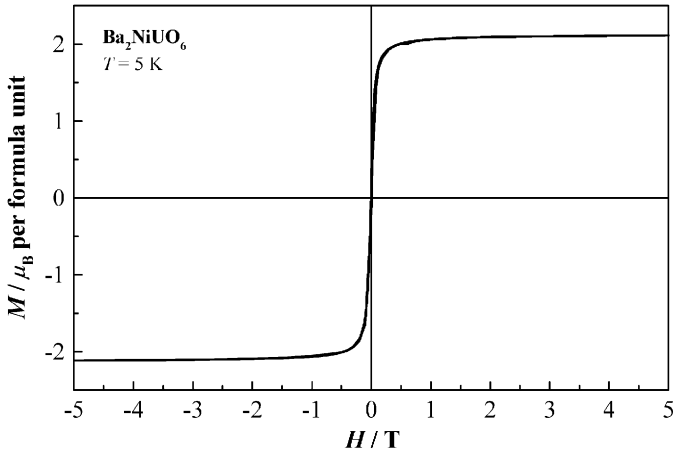

Fig. 8. Magnetic hysteresis curve for Ba_2NiUO_6 measured at 5 K.

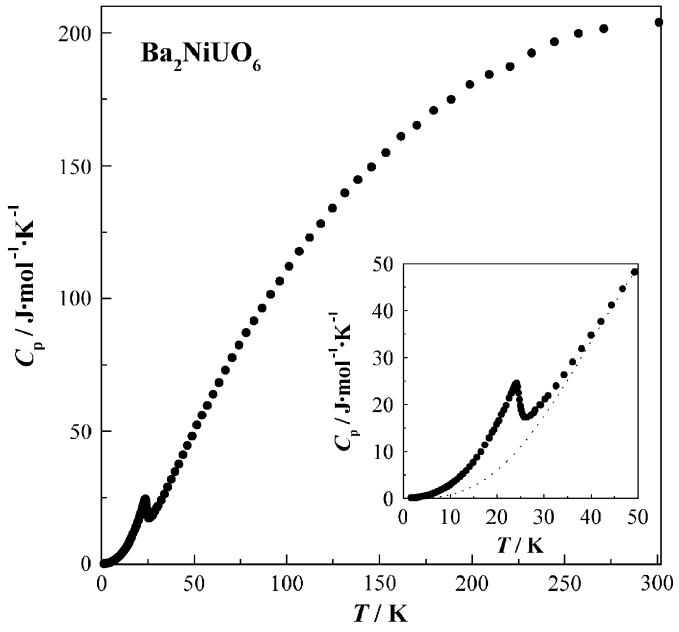

Fig. 9. Temperature dependence of the specific heat C_p for Ba_2NiUO_6. The inset shows the detailed temperature dependence below 40 K. The dotted line is the calculation results for the lattice specific heat (see text).

experimental specific heat. The variation of the magnetic specific heat divided by temperature (C_{mag}/T) against temperature is shown in Fig. 10. The temperature dependence of the magnetic entropy (S_{mag}) calculated by $S_{mag}(T) = \int (C_{mag}/T)dT$ is also shown in the same figure. The magnetic entropy change due to this ferromagnetic ordering of Ni^{2+} ions in the Ba_2NiUO_6 is obtained to be about 8.1 J/mol K. The comparable magnetic entropy change has been reported for NiU_2O_6 in which the Ni^{2+} ion is also in an octahedral crystal field environment and shows an antiferromagnetic transition at 35.6 K [35]. The result of the magnetic entropy change indicates that the degeneracy of the ground state for the Ni^{2+} ion in Ba_2NiUO_6 should be quadruple.

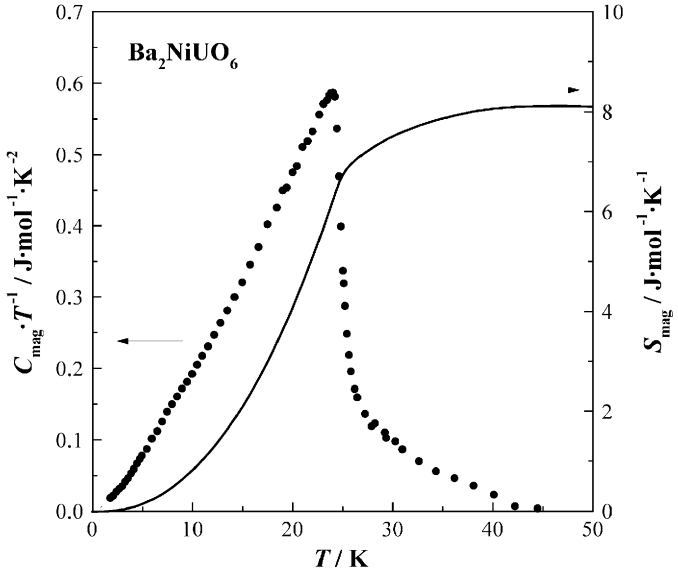

Fig. 10. Temperature dependences of the magnetic specific heat divided by temperature C_{mag}/T (left ordinate) and the magnetic entropy change S_{mag} (right ordinate) for Ba_2NiUO_6 below 50 K.

4. Summary

Uranium oxides Ba_2MUO_6 (M = Co, Ni) with the double perovskite structure were prepared. The Rietveld analysis shows that the structure was refined by applying the space group $Fm\bar{3}m$. This space group allows two crystallographically distinct octahedral sites in the ABO_3 perovskite structure, thus permitting 1:1 positional ordering between the B-site ions, U^{6+} and Co^{2+} (or Ni^{2+}) ions. Detailed magnetic susceptibility and specific heat measurements show that Ba_2CoUO_6 and Ba_2NiUO_6 are ordered ferromagnetically at 9.1 and 25 K, respectively.

Acknowledgments

This work was supported by Grant-in-aid for Scientific Research of Priority Areas "Panoscopic Assembling and High Ordered Functions for Rare Earth Materials" No. 17042003 from the Ministry of Education, Science, Sports, and Culture of Japan.

References

[1] K. Ito, K. Tezuka, Y. Hinatsu, J. Solid State Chem. 157 (2001) 173.
[2] M.T. Anderson, K.B. Greenwood, G.A. Taylor, K.R. Poeppelmeier, Prog. Solid State Chem. 22 (1993) 197.
[3] P.D. Battle, W.J. Macklin, J. Solid State Chem. 52 (1984) 138.
[4] P.D. Battle, C.W. Jones, J. Solid State Chem. 78 (1989) 108.
[5] P.D. Battle, C.W. Jones, R. Studer, J. Solid State Chem. 90 (1991) 302.
[6] E.M. Ramos, I. Alvarez, R. Saez-Puche, M.L. Veiga, C. Pico, J. Alloy Compd. 225 (1995) 212.
[7] Y. Doi, Y. Hinatsu, J. Phys.: Condens. Matter 11 (1999) 4813.
[8] M. Wakeshima, D. Harada, Y. Hinatsu, N. Masaki, J. Solid State Chem. 147 (1999) 618.
[9] K. Henmi, Y. Hinatsu, N. Masaki, J. Solid State Chem. 148 (1999) 353.

[10] M. Wakeshima, D. Harada, Y. Hinatsu, J. Mater. Chem. 10 (2000) 419.
[11] K. Tezuka, K. Henmi, Y. Hinatsu, N. Masaki, J. Solid State Chem. 154 (2000) 591.
[12] H.A. Blackstead, J.D. Dow, D.R. Harshman, W.B. Yelon, M.X. Chen, M.K. Wu, D.Y. Chen, F.Z. Chien, D.B. Pulling, Phys. Rev. B 63 (2001) 214412.
[13] Y. Doi, Y. Hinatsu, J. Phys.: Condens. Matter 13 (2001) 4191.
[14] R.H. Mitchell, Perovskites: Modern and Ancient, Almaz Press, Ont., Canada, 2002.
[15] Y. Sasaki, Y. Doi, Y. Hinatsu, J. Mater. Chem. 12 (2002) 2361.
[16] L. Li, B.J. Kennedy, J. Solid State Chem. 177 (2004) 3290.
[17] W.T. Fu, D.J.W. IJdo, J. Solid State Chem. 178 (2005) 1312.
[18] K.-I. Kobayashi, T. Kimura, H. Sawada, K. Terakura, Y. Tokura, Nature 395 (1998) 677.
[19] A. Maignan, B. Raveau, C. Martin, M. Hervieu, J. Solid State Chem. 144 (1999) 224.
[20] J.A. Alonso, M.T. Casais, M.J. Martinez-Lope, J.L. Martinez, P. Velasco, A. Munoz, M.T. Fernandez-Diaz, Chem. Mater. 12 (2000) 161.
[21] M.C. Viola, M.J. Martinez-Lope, J.A. Alonso, J.L. Martinez, J.M. De Paoli, S. Pagola, J.C. Pedregosa, M.T. Fernandez-Diaz, R.E. Carbonio, Chem. Mater. 15 (2003) 1655.
[22] R. Pinacca, M.C. Viola, J.C. Pedregosa, A. Munoz, J.A. Alonso, J.L. Martinez, R.E. Carbonio, Dalton Trans. 447 (2005).
[23] Y. Hinatsu, J. Alloy Compd. 215 (1994) 161.
[24] D.E. Cox, G. Shirane, B.C. Frazer, J. Appl. Phys. 38 (1967) 1459.
[25] F. Izumi, T. Ikeda, Mater. Sci. Forum 321–324 (2000) 198.
[26] R.D. Shannon, Acta Crystallogr. A 32 (1976) 751.
[27] I.D. Brown, in: M. O'Keeffe, A. Navrotsky (Eds.), Structure and Bonding in Crystals, vol. 1, Academic Press, New York, 1981.
[28] R.L. Carlin, Magnetochemistry, Springer, Berlin, 1986 (Chapter 4).
[29] E.F. Bertaut, A. Delapalme, F. Forrat, R. Pauthenet, J. Phys. Radium 23 (1962) 477.
[30] V.A. Bokov, S.A. Kizhaev, I.E. Myl'nikova, A.G. Tutov, Soviet Phys.—Solid State 6 (1965) 2419.
[31] J.E. Gordon, R.A. Fisher, Y.X. Jia, N.E. Phillips, S.F. Reklis, D.A. Wright, A. Zettle, Phys. Rev. B 59 (1999) 127.
[32] S.J. Joshua, A.P. Crackell, Phys. Lett. A 28 (1969) 562.
[33] A. Earnshaw, Introduction to Magnetochemistry, Academic Press, London, 1968.
[34] E. König, G. König, in: K.-H. Hellwege, A.M. Hellwege (Eds.), Landolt-Börnstein Tabellen, New Series, Group II, vols. 2, 8, 10–12, Magnetic Properties of Coordinated and Organometallic Transition Metal Compounds, Springer, Berlin, 1966, 1976, 1979, 1981, 1984.
[35] Y. Hinatsu, J. Solid State Chem. 114 (1995) 595.